Optimal Control of H-Mode Tokamak Plasma Temperature based on Pontryagin's Principle ⋆

S. Jmal * **M. Tacchi-Bénard** * **E. Witrant** *

* *CNRS, GIPSA-lab, Univ. Grenoble Alpes, 38000 Grenoble, France (e-mail: {slim.jmal, matteo.tacchi, emmanuel.witrant}@gipsa-lab.fr).*

Abstract: This paper studies the decay of an objective functional using a new control technique within Pontryagin's framework. Convergence analysis is carried out on the infinite-dimensional space of Tokamak plasma dynamical state as described by weakly decoupled nonlinear partial differential equations. An adjoint-based optimal control is derived to minimize the deviation from a predefined dynamical trajectory leading to the desired target state at stationary regime, by turning Pontryagin's transversality conditions into a continuum of horizons. A feedback controller is proposed to steer the system efficiently in real-time, as opposed to an open-loop controller resulting from the classical Pontryagin's setting. An algorithm synthesizing the constraint-free optimal controller is used for profile tracking based on experimental data.

Keywords: Thermonuclear fusion, nonlinear PDEs, H-mode Tokamak, Pontryagin's principle.

1. INTRODUCTION

Controlling electron temperature profiles in Tokamaks is essential for improving plasma confinement and ensuring stability in high-confinement regimes (H-mode), where elevated core temperatures significantly enhance confinement times Keilhacker (1987). Achieving stable temperature regulation remains a major challenge for future fusion reactors due to the nonlinear and distributed nature of plasma transport dynamics.

Various control strategies have been proposed for Tokamak plasma control. Early approaches relied on linearized and singular perturbation models Moreau et al. (2008), while more advanced works considered nonlinear first-principles formulations Moreau et al. (2013); Witrant et al. (2007). Distributed profile control has also been investigated through spatial discretization methods Felici (2011) and infinite-dimensional PDE-based formulations Boyer et al. (2013); Bribiesca Argomedo et al. (2013). More recently, reduced-order and data-driven approaches have been explored for coupled plasma dynamics Mavkov et al. (2017, 2018).

Parallel to that, optimal control of parabolic PDEs has been extensively developed within Pontryagin's Maximum Principle (PMP) framework in infinite-dimensional Hilbert spaces by Lions (1971); Barbu (1993); Tröltzsch (2010); Li and Yong (1991). While Casas et al. (2012); Aronna et al. (2021) extended the framework to include state-constraints and sparse controls, Tucsnak et al. (2016) did robustness analysis under perturbations, and Dubljevic et al. (2006); Hashimoto et al. (2012); Ito and Kunisch (2002) employed Model Predictive Control (MPC) strategies for distributed parameter systems.

Building upon these developments, this work proposes a receding-horizon reformulation of PMP for nonlinear parabolic PDEs governing Tokamak electron temperature diffusion. Instead of enforcing a single terminal target, we introduce a continuum of dynamically evolving reference states, yielding a closed-loop optimal control strategy with improved tracking and stabilization properties. The resulting framework preserves the infinite-dimensional PMP structure while integrating MPC-like feedback mechanisms, and is particularly suited for constrained distributed controls.

2. SYSTEM DESCRIPTION AND CONTROL PROBLEM

2.1 Electron Temperature Dynamics

The evolution of the electron temperature $T_e(x,t)$ is governed by a nonlinear parabolic PDE modeling heat transport in Tokamak plasmas. Under the assumption of toroidal symmetry, the system reduces to the 1D radial diffusion equation studied by Clémençon et al. (2004) in the cylindrical coordinate system with radial variable $x \in [0,1]$ and mixed Dirichlet and Neumann boundary conditions $T_e(1,t) = T_{edge}(t) \approx 0$, $\frac{\partial T_e}{\partial x}(0,t) = 0$, $\forall t \geq 0$

$$\frac{3}{2}\frac{\partial(n_e T_e)}{\partial t} = \frac{1}{a^2}\frac{1}{x}\frac{\partial}{\partial x}\left(x n_e \chi_e \frac{\partial T_e}{\partial x}\right) - P_{sink} + P_{sources} \quad (1)$$

$P_{sources}(x,t)$ includes external heating sources such as Ohmic heating (P_{OH}), Neutral Beam Injection and auxiliary power (P_{aux}) through radio frequency antennas. $P_{sink}(x,t)$ accounts for energy loss mechanisms, such as electron-ion equipartition losses and radiative cooling, which are often neglected in simplified models used by Witrant et al. (2007) Felici (2011).

⋆ Jmal et al. (2026)

2.2 Electron Heat Diffusivity Model

Semi-empirical models are employed instead of a fully analytic model for the electron heat diffusivity because of the complexity of plasma heat transport. In this work, we adopt an extended Bohm/gyro-Bohm model developed by Christofides and Chow (2002); Pianroj and Onjun (2012), and later successfully used by Mameche et al. (2019) in transport simulations of H-mode Tokamak plasmas.
The model expresses the electron heat diffusivity as

$$\chi_e = \chi_{ec} \times f_s, \quad \chi_{ec} = (2\chi_{Be} + \chi_{gBe}) f_s. \tag{2}$$

where the classical diffusivity χ_{e_c} is decomposed into Bohm and gyro-Bohm contributions. The latter writes

$$\chi_{gBe} = 5 \times 10^{-6} \sqrt{T_e} \left| \frac{\nabla T_e}{B_{\phi_0}^2} \right| \tag{3}$$

whereas the Bohm diffusivity is expressed as

$$\chi_{Be} = 4 \times 10^{-5} R \left| \frac{\nabla (n_e T_e)}{n_e B_{\phi_0}} \right| q^2 \left(\frac{T_{e,0.8} - T_{e,1}}{T_{e,1}} \right) \tag{4}$$

$T_{e,1}$ (resp $T_{e,0.8}$) represents the electron temperature at $x = 1$ (resp 0.8) and the last ratio represents the phenomena in which the diffusivity decreases when the edge temperature is increased.

The suppression function $f_s(x)$ accounts for the reduced transport due to turbulence stabilization mechanisms

$$f_s(x) = \frac{1}{1 + k \left(\frac{\omega_{E\times B}}{\gamma_{ITG}} \right)^2} \times \frac{1}{\max\left(1, (s - s_{thres})^2\right)} \tag{5}$$

This expression for f_s was derived based on experimental results by Pianroj and Onjun (2012); Sugihara et al. (2001) to ensure that a transport barrier -the pedestal- is properly modelled near the plasma edge.

Assumption 1. The semi-empirical diffusivity model used here relies on standard control-oriented assumptions, including slow temporal variations of the safety factor profile q compared to the electron temperature and time-averaged representations of density and loss-related coefficients

Decoupling the magnetic effects from the thermal ones for our PDE-based control problem and defining $A = 2/(3a^2)$, we formualte the diffusion coefficient as

$$\chi(x,t) = A\big(B(x) + C(x)\sqrt{T_e(x,t)}\big)\left|\nabla T_e(x,t)\right| \tag{6}$$

where

$$\begin{cases} B(x) = \dfrac{8 \times 10^{-5} R L_{T_e}}{B_{\phi_0}} q^2(x) f_s(x) \\ C(x) = \dfrac{5 \times 10^{-6}}{B_{\phi_0}^2} f_s(x) \end{cases} \tag{7}$$

and the constant L_{T_e} measures the time-averaged temperature gradient from $\big(T_e(0.8) - T_e(1)\big)/T_e(1)$.

2.3 Optimal Control Problem

We formulate our problem as an optimal control problem in the Pontryagin framework with a continuum of horizons, the time-discretization of which simplifies to the more classical MPC-like receding horizon control. The goal is to reach a desired electronic temperature profile $\bar{T}_e(x)$ for the Tokamak plasma by controlling the net input heating power $u(x,t)$, while ensuring stability of the system. The control law should not only minimize deviations from a dynamically evolving reference trajectory, but also be robust to errors due to inaccuracies in the model described by the dynamical equation

$$\begin{aligned} \frac{\partial T_e}{\partial t} &= \frac{A}{x}\frac{\partial}{\partial x}\left(x\big(B(x) + C(x)\sqrt{T_e}\big)\left(\frac{\partial T_e}{\partial x}\right)^2 \right) + u \\ &\overset{(6)}{=} \frac{1}{x}\frac{\partial}{\partial x}\left(x\chi\frac{\partial T_e}{\partial x} \right) + u \end{aligned} \tag{8}$$

The optimal control problem (OCP) then formulates as the PDE-constrained minimization problem of the distance to a predefined, dynamical trajectory leading to the final-time target at $t_f < \infty$, plus a regularity constraint on the $L^2_x = L^2(xdx)$-norm of the control variable

$$\min_{\substack{T_e \in \mathcal{A} \\ u \in \mathcal{U}}} \left[\int_0^{t_f} \left(\mathcal{J}_1(t, u, T_e[u]) + \frac{\alpha(t)}{2} \|u\|^2_{L^2_x} \right) dt \right] \tag{9}$$

where $\mathcal{A}$ is the set of admissible solutions to equation (8), and $\mathcal{U}$ is the admissible control space, assumed only to be $H^1([0,1])$. The set of intermediate cost functionals $(\mathcal{J}_1(t,\cdot,\cdot))_{t\in[0,t_f]}$ and penalizing terms $(\alpha(t))_{t\in[0,t_f]}$ are detailed in the following sections.

3. A PONTRYAGIN-BASED APPROACH

3.1 Receding Horizon Pontryagin's Principle

Pontryagin's classical setting with one end-point horizon has the inconvenience of providing an open-loop optimal controller independently from the real evolution of the system. It is therefore prone to errors due to numerical instabilities and deviations of the model from reality. Extending it through a smooth continuum of horizons could prevent these problems by providing a feedback optimal controller in a closed-loop with the system. Let the intermediate targets $(\hat{T}_e(\cdot,t))_{t\in[0,t_f]}$ define our receded horizons as an exponential interpolation between the initial state $T_{e,0}(\cdot)$ and the final-time target $\bar{T}_e(\cdot)$

$$\hat{T}_e(x,t) = T_{e,0}(x) + (1 - e^{-\mu t/t_f})\big(\bar{T}_e(x) - T_{e,0}(x)\big) \tag{10}$$

The corresponding intermediate cost functional measuring the distance of the controlled state to that intermediate target is

$$\mathcal{J}_1(t, u, T_e[u]) = \frac{1}{2}\int_0^1 \big(T_e(x,t) - \hat{T}_e(x,t)\big)^2 x dx \tag{11}$$

Given a partition $(t_i)_i$ of the time interval $[0, t_f]$, we reformulate OCP (9) into subproblems of optimal control bringing up the structure of the classical Pontryagin setting in open-loop. Suppose indeed that we controlled the system up to a time $[0, t_f[\ni t_i =: t$ along the reference trajectory $\hat{T}_e$. Set the new time horizon $\tau := t_{i+1} \in]t_i, t_f]$

$$\min_{\substack{T_e \in \mathcal{A} \\ u \in \mathcal{U}}} \left[\mathcal{J}_1(\tau, u, T_e[u]) + \frac{\alpha(\tau)}{2}\|u\|^2_{L^2_x} \right] \tag{12}$$

Solving this subproblem of optimal control within Pontryagin's framework requires the introduction of an augmented Lagrangian $\mathcal{L}$ via the Lagrange multiplier p:

$$\begin{aligned} \mathcal{L}(\tau, u, T_e, p) &\overset{\text{def}}{=} \mathcal{J}_1(\tau, u, T_e) + \frac{\alpha(\tau)}{2}\int_t^\tau \int_0^1 u(x,t)^2 x\, dx \\ &+ \left\langle p, \underbrace{\frac{1}{x}\frac{\partial}{\partial x}\left(x\chi\frac{\partial T_e}{\partial x}\right) + u - \frac{\partial T_e}{\partial t}}_{\overset{=}{(8)} 0} \right\rangle_{L^2_x} \end{aligned} \tag{13}$$

Separately calculating the PDE-constraint enforcing term

$$\left\langle p, \frac{1}{x}\frac{\partial}{\partial x}\Big(x\chi\frac{\partial T_e}{\partial x}\Big) + u - \frac{\partial T_e}{\partial t}\right\rangle_{L_x^2} = \int_t^\tau \int_0^1 pu\, xdxdt$$

$$+ \int_t^\tau \cancel{x\chi p\frac{\partial T_e}{\partial x}\Big|_0^1} dt - \int_t^\tau \int_0^1 \chi\frac{\partial p}{\partial x}\frac{\partial T_e}{\partial x}\, xdxdt \tag{14a}$$

$$+ \int_t^\tau \int_0^1 \frac{\partial p}{\partial t}T_e\, xdxdt - \int_0^1 p(x,\tau)T_e(x,\tau)\, xdx \tag{14b}$$

$$+ \int_0^1 p(x,t)T_e(x,t)\, xdx \tag{14c}$$

where (14a) expands the term $\langle p, \frac{1}{x}\frac{\partial}{\partial x}(x\chi\frac{\partial T_e}{\partial x})\rangle_{L_x^2}$ and (14b)-(14c) expand the term $\langle p, -\frac{\partial T_e}{\partial t}\rangle_{L_x^2}$, both via integration by parts. The boundary term vanishes thanks to the homogeneous Neumann boundary condition $\frac{\partial T_e}{\partial x}(0,\cdot) = 0$ and by enforcing Dirichlet boundary condition $p(1,\cdot) = 0$ on the costate.

By the homogeneous Dirichlet boundary condition $T_e(1,\cdot) = 0$, expression (14a) further simplifies into this form

$$-\int_t^\tau \int_0^1 \chi\frac{\partial p}{\partial x}\frac{\partial T_e}{\partial x}\, xdxdt = -\int_t^\tau \cancel{x\chi\frac{\partial p}{\partial x}T_e\Big|_0^1} dt$$

$$+ \int_t^\tau \int_0^1 \frac{\partial}{\partial x}\Big(x\chi\frac{\partial p}{\partial x}\Big)T_e\, dxdt. \tag{15}$$

Bringing together all the members of equation (13), we get the final expression of the augmented Lagrangian

$$\mathcal{L}(\tau, u, T_e, p) = \int_t^\tau \int_0^1 \Big[pu + \frac{\alpha}{2}u^2\Big]\, xdxdt \tag{16}$$

$$+ \int_0^1 \Big[\frac{1}{2}\big(T_e(x,\tau) - \hat{T}_e(x,\tau)\big)^2 - p(x,\tau)T_e(x,\tau)\Big]\, xdx$$

$$+ \int_t^\tau \int_0^1 \Big[\frac{\partial p}{\partial t} + \frac{1}{x}\frac{\partial}{\partial x}\Big(x\chi\frac{\partial p}{\partial x}\Big)\Big]T_e\, xdxdt$$

$$+ \int_0^1 p(x,t)T_e(x,t)\, xdx$$

Remark 1. The last term is irrelevant to our optimization, since it no longer is a horizon but a given "initial condition" for the optimal control problem on the interval $[t,\tau]$.

At this stage, variations of the Lagrangian will be taken with respect to the triplet state-costate-control (T_e, p, u). For computational simplicity, we assume that the diffusivity is state-independent $\frac{\partial\chi}{\partial T_e} = 0$ over the small horizon $[t,\tau]$, since the nonlinear-dependency terms are very small $(B(x), C(x) \ll 1)$. Now we set the Lagrangian stationary with respect to the state

$$0 = \begin{pmatrix}\nabla_{T_e(\cdot,\cdot)}\mathcal{L}\\ \nabla_{T_e(\cdot,\tau)}\mathcal{L}\end{pmatrix} \tag{17}$$

rewrites as the adjoint equation

$$\begin{cases}\dfrac{\partial p}{\partial t} = -\dfrac{1}{x}\dfrac{\partial}{\partial x}\Big(x\chi\dfrac{\partial p}{\partial x}\Big), & \text{a.e. on } [0,1]\times[t,\tau]\\ p(x,\tau) = T_e(x,\tau) - \hat{T}_e(x,\tau), & \text{a.e. in } [0,1]\end{cases} \tag{18}$$

with Dirichlet boundary condition $p(1,\cdot) = 0$ as stated above. Making the Lagrangian stationary with respect to the control yields Pontryagin's optimality condition

$$0 = \nabla_u\mathcal{L} = p + \alpha(\tau)u \tag{19}$$

Injecting (18)-(19) back into the state equation (8) yields the coupled state-costate PDE system on $[0,1]\times[t,\tau]$

$$\begin{cases}\dfrac{\partial T_e}{\partial t} = \dfrac{1}{x}\dfrac{\partial}{\partial x}\Big(x\chi\dfrac{\partial T_e}{\partial x}\Big) - \dfrac{1}{\alpha}p\\ \dfrac{\partial p}{\partial t} = -\dfrac{1}{x}\dfrac{\partial}{\partial x}\Big(x\chi\dfrac{\partial p}{\partial x}\Big)\end{cases} \tag{20}$$

and the following initial-final conditions

$$\begin{cases}T_e(\cdot,t) = T_{e,t}(\cdot)\\ p(\cdot,\tau) = T_e(\cdot,\tau) - \hat{T}_e(\cdot,\tau).\end{cases} \tag{21}$$

Except for the transversality conditions, notice that PMP does not depend on the time horizon choice, so we differentiate the former by making δt arbitrarily small

$$\begin{aligned}\frac{\partial p}{\partial t} &= \lim_{\delta t\to 0}\frac{p(\cdot,t+\delta t) - p(\cdot,t)}{\delta t}\\ &= \lim_{\tau\downarrow t}\frac{\big(T_e(\cdot,\tau) - \hat{T}_e(\cdot,\tau)\big) - \big(T_e(\cdot,t) - \hat{T}_e(\cdot,t)\big)}{\tau - t}\\ &= \frac{\partial T_e}{\partial t} - \frac{\partial\hat{T}_e}{\partial t}.\end{aligned} \tag{22}$$

Substituting (22) back into the state-costate PDEs (20):

$$-\frac{1}{x}\frac{\partial}{\partial x}\Big(x\chi\frac{\partial p}{\partial x}\Big) = \frac{1}{x}\frac{\partial}{\partial x}\Big(x\chi\frac{\partial T_e}{\partial x}\Big) - \frac{1}{\alpha}p - \frac{\partial\hat{T}_e}{\partial t} \tag{23}$$

hence the inverse problem on the adjoint variable p

$$\Big(\frac{1}{\alpha}Id - \frac{1}{x}\frac{\partial}{\partial x}\Big(x\chi\frac{\partial}{\partial x}\Big)\Big)p = \frac{1}{x}\frac{\partial}{\partial x}\Big(x\chi\frac{\partial T_e}{\partial x}\Big) - \frac{\partial\hat{T}_e}{\partial t}. \tag{24}$$

Combining both transversality and stationarity conditions into this quasi-steady solution for the adjoint state, we bypass the difficulty of solving it backward in time as in the original one-end horizon formulation.

We derived a closed-loop optimal controller evolving forward in time alongside the controlled state, guiding the system along a reference trajectory toward the final target and enabling real-time error corrections by feedback.

3.2 Convergence Analysis

We want to prove convergence of the controlled state toward the final target, which is measured by the objective functional

$$\mathcal{J}(t) = \frac{1}{2}\int_0^1 \big(T_e(x,t) - \bar{T}_e(x)\big)^2\, xdx \tag{25}$$

Inserting the intermediate target $\hat{T}_e(\cdot,t)$ between both terms and using the definition of $\hat{T}_e(\cdot,t_f)$

$$\mathcal{J}(t) = \frac{1}{2}\int_0^1 \Big(\big(T_e(x,t) - \hat{T}_e(x,t)\big) + \big(\hat{T}_e(x,t) - \hat{T}_e(x,t_f)\big)\Big)^2\, xdx \tag{26}$$

By virtue of the classical arithmetic–geometric inequality

$$\mathcal{J}(t) \le 2\big(\mathcal{J}_1(t) + \mathcal{J}_2(t)\big) \tag{27}$$

where the two functionals $\mathcal{J}_1$ and $\mathcal{J}_2$ are defined as

$$\begin{cases}\mathcal{J}_1(t) = \dfrac{1}{2}\displaystyle\int_0^1 \big(T_e(x,t) - \hat{T}_e(x,t)\big)^2\, xdx\\ \mathcal{J}_2(t) = \dfrac{1}{2}\displaystyle\int_0^1 \big(\hat{T}_e(x,t) - \hat{T}_e(x,t_f)\big)^2\, xdx\end{cases} \tag{28}$$

Trivially, we see that the second term $\mathcal{J}_2$ is exponentially decaying. Indeed, plugging in the expression of the reference trajectory $\hat{T}_e$ as an exponential interpolation gives

$$\begin{aligned}\mathcal{J}_2(t) &= \frac{1}{2}\int_0^1 \left(\hat{T}_e(x,t) - \hat{T}_e(x,t_f)\right)^2 x dx \\ &= \frac{1}{2}\int_0^1 e^{-2\mu t/t_f}\left(\hat{T}_e(x,0) - \hat{T}_e(x,t_f)\right)^2 x dx \\ &= e^{-2\mu t/t_f}\mathcal{J}_2(0), \quad t \in [0,t_f]\end{aligned} \tag{29}$$

As for the first term $\mathcal{J}_1$, we will show that it remains small thanks to our optimization-based control method, aiming at minimizing the deviation of the controlled state from a given reference trajectory by calibrating in real-time the parameter $\alpha(t)$ based on the evolution of $\mathcal{J}_1(t)$ itself.

More specifically, we want to establish an empirical law governing the penalty term $\alpha(t)$ of the form

$$\dot{\alpha}(t) = \beta(t) \times h(\mathcal{J}_1(t), \dot{\mathcal{J}}_1(t)) \tag{30}$$

where $\beta \in \{-1, 1\}$ is the adjustment sign to compensate overshooting or undershooting a midway-target, defined as

$$\beta(t) = \text{sign}\left(\int_0^1 \left(T_e(x,t) - \hat{T}_e(x,t)\right) x dx\right) \tag{31}$$

and $h \geq 0$ measures the strength of the deviation of $\mathcal{J}_1$ from 0 as detailed below. Intuitively, if $T_e(\cdot,t)$ is above the midway-target $\hat{T}_e(\cdot,t)$ on average , the sign is positive and we amplify the regularity constraint on the control, otherwise we relax it.

To study the effect of α, we intend to calibrate it once using the standard one-horizon Pontryagin setting on the whole time interval $[0,t_f]$ instead of $[t,\tau]$ as developed in Section 3.1. We retrieve the same adjoint equation (18) but on $[0,1] \times [0,t_f]$ alongside Pontryagin's optimality conditions (19) leading to the coupled state-costate PDEs (20) with initial conditions at time $t = 0$ and transversality conditions at final time $\tau = t_f$.

Solving the above coupled PDEs for a constant penalty term α gives us the optimal energy $\mathcal{J}^*(\alpha) = \mathcal{J}(u^*, T_e^*, p^*)$ at the optimal triplet (u^*, T_e^*, p^*) solution to PMP with α-regularized Lagrangian $\mathcal{L}$. Doing the same for different values of α allows us to heuristically analyse the variations of $\mathcal{J}^*$ with respect to α around the optimal penalty term $\alpha^* = \arg\min_\alpha \mathcal{J}^*(\alpha)$.

The following quadratic relation best approximates the results obtained from numerical experimentations

$$\mathcal{J}^*(\alpha) = \kappa(\alpha - \alpha^*)^2, \quad \kappa > 0 \tag{32}$$

This empirical relation is valid for a classical one-horizon Pontryagin framework at a fixed time. Extending it to our continuum of horizons setting requires further assumptions on the coefficient κ and the evolving optimal regularizing parameter, that is their time-invariability $\kappa(t) = \kappa$ and $\alpha^*(t) = \alpha^*$

$$\mathcal{J}_1(\alpha(t)) = \kappa(\alpha(t) - \alpha^*)^2 \tag{33}$$

Under these hypothesises, we derive the empirical formula

$$\begin{aligned}\dot{\mathcal{J}}_1(t) = \frac{d}{dt}\mathcal{J}_1(\alpha(t)) &= \frac{\partial \mathcal{J}_1}{\partial \alpha} \cdot \dot{\alpha}(t) \\ &\overset{(33)}{=} 2\kappa(\alpha(t) - \alpha^*) \cdot \dot{\alpha}(t) \\ &\overset{(31)}{=} 2\beta\sqrt{\kappa}\sqrt{\mathcal{J}_1(t)} \cdot \dot{\alpha}(t) \\ \Rightarrow |\dot{\alpha}(t)| = h(\mathcal{J}_1, \dot{\mathcal{J}}_1) &\propto \frac{\dot{\mathcal{J}}_1(t)}{\sqrt{\mathcal{J}_1(t)}}\end{aligned} \tag{34}$$

By including this adaptive feedback mechanism for the regularizing parameter in our algorithm, we complete the synthesis of the optimal control law.

4. CONTROL ALGORITHM IMPLEMENTATION AND SIMULATION RESULTS

4.1 Control Algorithm

The proposed adjoint-based optimal control algorithm, is specifically tuned to conform with the H-mode configuration of Tore Supra Tokamak for tracking a desired electronic temperature profile $\bar{T}_e$. Simulation results are presented in Subsection 4.2 below.

4.2 Simulation Results

All numerical simulations are performed by taking into account the model presented in Subsection 2.2, where the parameters of the heat diffusivity are calibrated on experimental measurements extracted from the Tore Supra shot 36 056 (12/08/2005) obtained with lower hybrid (2.5 MW) and ion cyclotron (5 MW) radio frequency antennas. The free parameters used in Subsection 3.1 are as follows: the final time is set to $t_f = 1$, and the exponentiation parameter in the expression of the reference trajectory is fixed at $\mu = 5.85$ for an abrupt ramp-up phase at the start of the plasma heating.

Figure 1 depicts the space-time evolution of the controlled plasma temperature $T_e(x,t)$ along the prescribed reference trajectory $\hat{T}_c(x,t)$, which was defined as an exponential interpolation connecting the initial state to the experimentally identified stationary target corresponding to the Tore Supra optimal H-mode equilibrium.

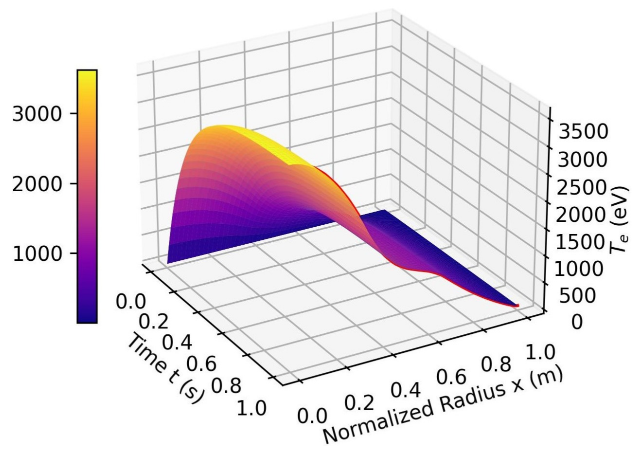

Fig. 1. Controlled Plasma Temperature Evolution

The controlled dynamics remain nearly indistinguishable from the reference trajectory, demonstrating the high fidelity of the control strategy in tracking the desired temperature evolution. Figure 2 further confirms that the controlled temperature profile almost-perfectly matches the final-time target with a discrepancy of $1.01 \cdot 10^{-7}$.

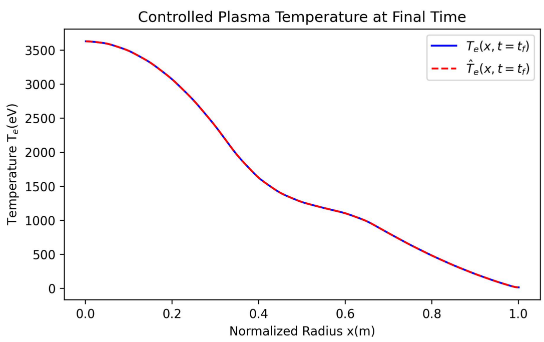

Fig. 2. Controlled Plasma Temperature at Final Time

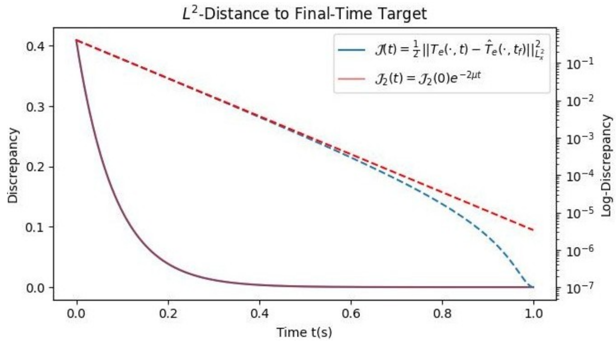

Fig. 4. Convergence of the Objective Functional

The exponential speed of convergence is essentially the same as that imposed on the controlled system through the reference trajectory, until orders of magnitudes below where tiny deviations play out due to control-induced minimization of the first bounding term in inequality (27).

Figure 5 below showcases the evolution of J_1 as a measure of deviation from predefined intermediate targets, topping out at $3.369 \cdot 10^{-6}$ by the end of the control process

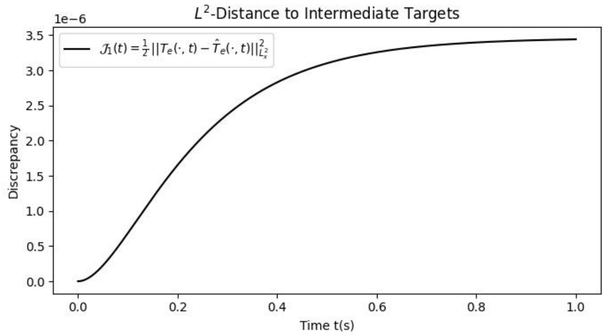

Fig. 5. Tracking the Reference Trajectory

The space–time distribution of the optimal power input in Figure 3 clearly illustrates the physically expected shape of auxiliary heating in an H-mode Tokamak discharge: an initial, sharp energy deposition localized near the plasma core efficiently triggers the transition to high confinement, while the required power rapidly decreases as the temperature gradient self-sustains through improved confinement. This behavior reproduces the typical pattern observed in high-performance discharges, where feedback actuators operate predominantly during the transient phase.

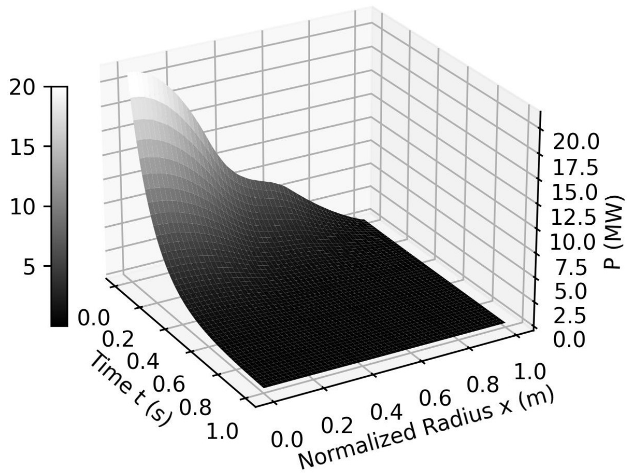

Fig. 3. Optimal Power Input Control Law

As studied in Subsection 3.2, the convergence analysis is further supported by the plots in Figure 4: two almost-overlapping curves; that of the exponentially decaying reference trajectory in red and that of the main objective functional in blue nearly fitting the former up to a small deviation due to our optimization-based control technique, as rendered more clearly visible on their log-scaled dotted counterparts.

These deviations have been controlled to be as small as possibly allowed by our regularized optimization-based control within Pontryagin's framework, while blending the adaptive law of the regularizating α-parameter into our control algorithm.

5. CONCLUSION

In this work, we introduced an optimal control strategy for fusion plasma dynamics governed by nonlinear PDEs of inhomogeneous diffusion type. The proposed methodology extends the classically open-loop Pontryagin framework into a feedback control mechanism by reformulating the transversality conditions as a continuum of receding intermediate targets, in the spirit of RHC. A closed-loop control law is derived by combining the PMP equations with an adaptive regularization of the control energy norm, ensuring convergence of a performance criterion measuring the deviation of the controlled state from a desired dynamical trajectory. This reformulation enables the systematic conversion of an open-loop optimal control problem into a feedback mechanism, allowing real-time compensation for modeling uncertainties and enhanced robustness with respect to external perturbations. Numerical results were obtained using a control algorithm based on the Bohm/gyro-Bohm transport model and calibrated on the H-mode plasma temperature diffusion of the Tore Supra tokamak. These simulations confirm the effectiveness and energetic efficiency of the proposed strategy for temperature profile tracking. Future investigations will incorporate geometric shape constraints and explore real-time implementation on platforms such as TCV's RAPTOR simulator, with a view toward scalability and integration in reactor-scale devices including ITER.

ACKNOWLEDGEMENTS

This work has been carried out within the framework of the EUROfusion Consortium, funded by the European Union via the Euratom Research and Training Programme (Grant Agreement No 101052200 - EUROfusion). Views and opinions expressed are however those of the author(s) only and do not necessarily reflect those of the European Union or the European Commission. Neither the European Union nor the European Commission can be held responsible for them. The work of Slim Jmal is supported by the program "Initiatives de Recherche à Grenoble Alpes" through the grant SOS-Fusion.

REFERENCES

Aronna, M.S., Bonnans, J.F., and Kröner, A. (2021). State constrained control-affine parabolic problems ii: second order sufficient optimality conditions. *SIAM Journal on Control and Optimization*, 59(2), 1628–1655.

Barbu, V. (1993). *Analysis and Control of Nonlinear Infinite Dimensional Systems*. Academic Press, Boston.

Boyer, M.D., Barton, J., Schuster, E., Luce, T.C., Ferron, J.R., Walker, M.L., Humphreys, D.A., Penaflor, B.G., and Johnson, R.D. (2013). First-principles-driven model-based current profile control for the DIII-D tokamak via lqi optimal control. *Plasma Physics and Controlled Fusion*, 55(10), 105007.

Bribiesca Argomedo, F., Witrant, E., Prieur, C., Brémond, S., Nouailletas, R., and Artaud, J.F. (2013). Lyapunov-based distributed control of the safety-factor profile in a tokamak plasma. *Nuclear Fusion*, 53(3), 033005.

Casas, E., Herzog, R., and Wachsmuth, D. (2012). Sparse solutions to linear pdes in optimal control. *SIAM Journal on Control and Optimization*, 50(4), 1735–1752.

Christofides, P.D. and Chow, J. (2002). Nonlinear and robust control of pde systems: Methods and applications to transport-reaction processes. *Appl. Mech. Rev.*, 55(2), B29–B30.

Clémençon, A., Guivarch, C., Eury, S., Zou, X., and Giruzzi, G. (2004). Analytical solution of the diffusion equation in a cylindrical medium with step-like diffusivity. *Physics of Plasmas*, 11(11), 4998–5009.

Dubljevic, S., El-Farra, N.H., Mhaskar, P., and Christofides, P.D. (2006). Predictive control of parabolic pdes with state and control constraints. *International Journal of Robust and Nonlinear Control: IFAC-Affiliated Journal*, 16(16), 749–772.

Felici, F. (2011). *Real-time control of tokamak plasmas: from control of physics to physics-based control*. Ph.D. thesis, EPFL.

Hashimoto, T., Yoshioka, Y., and Ohtsuka, T. (2012). Receding horizon control with numerical solution for nonlinear parabolic partial differential equations. *IEEE Transactions on Automatic Control*, 58(3), 725–730.

Ito, K. and Kunisch, K. (2002). Receding horizon optimal control for infinite dimensional systems. *ESAIM: control, optimisation and calculus of variations*, 8, 741–760.

Jmal, S., Tacchi-Bénard, M., and Witrant, E. (2026). Optimal control of h-mode tokamak plasma temperature based on pontryagin's principle. *Control Engineering Practice*, 172, 106919.

Keilhacker, M. (1987). H-mode confinement in tokamaks. *Plasma Physics and Controlled Fusion*, 29(10A), 1401.

Li, X. and Yong, J. (1991). Necessary conditions for optimal control of distributed parameter systems. *SIAM Journal on Control and Optimization*, 29(4), 895–908.

Lions, J.L. (1971). *Optimal control of systems governed by partial differential equations*, volume 170. Springer.

Mameche, H., Witrant, E., and Prieur, C. (2019). Nonlinear pde-based control of the electron temperature in h-mode tokamak plasmas. In *2019 IEEE 58th Conference on Decision and Control (CDC)*, 3227–3232. IEEE.

Mavkov, B., Witrant, E., and Prieur, C. (2017). Distributed control of coupled inhomogeneous diffusion in tokamak plasmas. *IEEE Transactions on Control Systems Technology*, 27(1), 443–450.

Mavkov, B., Witrant, E., Prieur, C., Maljaars, E., Felici, F., Sauter, O., et al. (2018). Experimental validation of a lyapunov-based controller for the plasma safety factor and plasma pressure in the tcv tokamak. *Nuclear Fusion*, 58(5), 056011.

Moreau, D., Mazon, D., Ariola, M., De Tommasi, G., Laborde, L., Piccolo, F., Sartori, F., Tala, T., Zabeo, L., Boboc, A., et al. (2008). A two-time-scale dynamic-model approach for magnetic and kinetic profile control in advanced tokamak scenarios on jet. *Nuclear Fusion*, 48(10), 106001.

Moreau, D., Walker, M.L., Ferron, J.R., Liu, F., Schuster, E., Barton, J.E., Boyer, M.D., Burrell, K.H., Flanagan, S., Gohil, P., et al. (2013). Integrated magnetic and kinetic control of advanced tokamak plasmas on DIII-D based on data-driven models. *Nuclear Fusion*, 53(6), 063020.

Pianroj, Y. and Onjun, T. (2012). Simulations of h-mode plasmas in tokamak using a complete core-edge modeling in the baldur code. *Plasma Science and Technology*, 14(9), 778.

Sugihara, M., Igitkhanov, Y., Janeschitz, G., Pacher, G., Pacher, H., Pereverzev, G., and Zolotukhin, O. (2001). Simulation studies on h-mode pedestal behavioru during type-i elms under various plasma conditions. In *Proceedings of the 28th EPS Conference on Controlled Fusion and Plasma Physics, Funchal, Portugal*, 629–632.

Tröltzsch, F. (2010). *Optimal control of partial differential equations: theory, methods, and applications*, volume 112. American Mathematical Soc.

Tucsnak, M., Wang, G., and Wu, C.T. (2016). Perturbations of time optimal control problems for a class of abstract parabolic systems. *SIAM Journal on Control and Optimization*, 54(6), 2965–2991.

Witrant, E., Joffrin, E., Brémond, S., Giruzzi, G., Mazon, D., Barana, O., and Moreau, P. (2007). A control-oriented model of the current profile in tokamak plasma. *Plasma Physics and Controlled Fusion*, 49(7), 1075.